



## Journal of Advanced Research in Applied Sciences and Engineering Technology

Journal homepage:  
[https://semarakilmu.com.my/journals/index.php/applied\\_sciences\\_eng\\_tech/index](https://semarakilmu.com.my/journals/index.php/applied_sciences_eng_tech/index)  
ISSN: 2462-1943



# Design And Optimization of A Cyclonic Mild Combustion Chamber Fueled by Producer Gas

Omar Al Rifai<sup>1,2</sup>, Khaled Ali Al-attab<sup>2,\*</sup>, Ibrahim Idris Enagi<sup>3,4</sup>, Khairil Faizi Mustafa<sup>2</sup>, Abdul Rahman Mohamed<sup>4</sup>

- <sup>1</sup> Mechanical Engineering Department, Australian University, School of Engineering, West Mishref, Kuwait  
<sup>2</sup> School of Mechanical Engineering, Universiti Sains Malaysia, Engineering Campus, 14300 Nibong Tebal, Penang, Malaysia  
<sup>3</sup> Department of Mechanical Engineering, School of Engineering Technology, Federal Polytechnic, P.M.B 55, Bida, Niger State -Nigeria  
<sup>4</sup> School of Chemical Engineering, Universiti Sains Malaysia, Engineering Campus, 14300 Nibong Tebal, Penang, Malaysia

### ARTICLE INFO

#### Article history:

Received 10 April 2026  
Received in revised form 18 May 2026  
Accepted 10 June 2026  
Available online 6 July 2026

#### Keywords:

MILD combustion; Biomass producer gas; Combustion chamber design; Computational fluid dynamics CFD; ANSYS-Fluent; Design of Experiments (DoE); Response optimizer

### ABSTRACT

Moderate or Intense Low-Oxygen Dilution (MILD) combustion offers a promising sustainable alternative energy resource, potentially bringing us closer to achieving net-zero emissions. However, limited research on MILD combustion technology means our understanding of its operation and integration into existing systems is still developing. The application of MILD combustion to low-grade biomass producer gas (PG) is particularly underexplored, with only a few studies conducted sporadically. This study aims to design and optimize a compact combustion chamber capable of achieving MILD combustion using low-grade PG, utilizing CFD simulations to assess key performance indicators such as maximum temperature rise ( $\Delta T$ ), Damköhler number ( $Da$ ), along with (CO) and (NO<sub>x</sub>) emissions. Two stages of Design of Experiments (DoE) were conducted: the first focused on optimizing the chamber's geometry, and the second on optimizing the swirler's geometry. A total of 18 CFD simulation cases were analysed using a full-factorial DoE to identify the variables that significantly influence MILD combustion and to determine the optimal design. From DoE 1, it was determined that the optimal chamber geometry has a width of 200 mm and a length of 1000 mm, as this configuration increases the chamber volume, thereby enhancing residence time and promoting better mixing of reactants. DoE 2 concluded that the optimal swirler geometry features a swirler angle ( $\Theta$ ) of 30° and eight blades (N), which generates a stronger vortex field within the chamber, improving fuel-air mixing. The final optimal design achieved CO emissions of 0.74 ppm, NO<sub>x</sub> emissions of 15.46 ppm,  $Da$  of 0.299, and  $\Delta T$  of 333.5°C.

## 1. Introduction

Shortly, fossil fuel combustion is expected to remain the dominant global energy source. However, as Capellán-Pérez *et al.*, [1] suggest, by 2032, there will be a significant gap between the

\* Corresponding author.  
E-mail address: [khaled@usm.my](mailto:khaled@usm.my)

supply and demand for fossil fuels. This imbalance will likely cause demand to surge as supplies dwindle, potentially leading to the depletion of fossil fuel reserves by 2042, as projected by Shafiee and Topal [2]. This situation is driven by the growing global population and the rapid economic development in many emerging economies. Although there has been a notable increase in renewable energy generation, 45% by China and 15% by the EU as of mid-2023, over half of the world still relies heavily on fossil fuels for energy, making them a critical factor in global growth and development [3]. The downside to this reliance is that fossil fuels are not environmentally sustainable, highlighting the urgent need to develop more efficient and less polluting combustion technologies, ideally utilizing alternative fuel sources.

One such alternative to fossil fuels is producer gas (PG), a by-product of gasification processes involving either the upward blowing of a steam and air mixture through a coal bed or biomass combustion in an oxygen-deficient environment with controlled moisture [4]. The resulting gas, known as PG, primarily consists of a mixture of carbon monoxide (CO), hydrogen (H), and nitrogen (N) generated from the chemical reactions during the process. This suggests that biomass-derived PG could serve as a green alternative to fossil fuels. Biomass, being a carbon-neutral renewable energy source, is derived from organic materials such as crop waste, livestock waste, and municipal waste. This makes it particularly advantageous for agricultural countries like Malaysia and others in Southeast Asia to explore and utilize their biomass resources such as empty fruit bunches, rice husks, and fruit fibres as renewable energy sources.

The combustion of low-grade producer gas (PG) was also examined in a cyclone reactor by Al-Attab [5], where stable combustion and acceptable NO<sub>x</sub> and CO emissions were achieved, however axial factorial optimization was adopted in the study. Zhien [6] also employed an axial factorial Design of Experiments (DoE) approach to investigate the combustion of low-grade producer gas (PG) in a staged combustor, focusing on the impact of various geometric manipulative variables. However, biomass-derived PG is not without its challenges. Due to its high concentration of CO, PG can pose toxic hazards under certain conditions (Food and Agriculture Organization (FAO), 1986). Additionally, the dilution of CO<sub>2</sub> and N<sub>2</sub> in PG results in a low heating value (LHV) ranging from 4–6 MJ/m<sup>3</sup>, necessitating improved fuel-air mixing at the molecular level and longer residence times to ensure complete combustion of the low-grade PG [7]. Consequently, low-grade PG combustion requires a larger combustion chamber to facilitate effective burning. Moreover, although PG is an environmentally friendly alternative, it is known for its instability and low combustion temperatures [6].

A relatively new combustion technique called Moderate or Intense Low-oxygen Dilution (MILD) combustion, also known as flameless oxidation (FLOX), can be implemented to address these issues. This technique is recognized for enhancing combustion efficiency while reducing pollutant emissions [8]. MILD combustion achieves these benefits by preheating the reactants, either through priming or adopting an exhaust gas recirculation (EGR) system—to counteract the low LHV of PG. Zhien [6] investigated an innovative combustor design that integrated three combustion concepts—swirl vane, cyclonic, and staged combustion—to enable efficient PG combustion within a compact geometry. The Design of Experiments (DoE) approach was utilized to optimize the combustor's geometric configuration.

Challenges of PG utilization as a fuel lie in its low quality, particularly when derived from biomass air-gasification, which results in an LHV as low as 4MJ/m<sup>3</sup> and a high dilution of non-combustible gases like N<sub>2</sub> and CO<sub>2</sub> that can exceed 50% of the total gas volume. Therefore, alternative methods are needed to achieve efficient and complete combustion of PG. One potential solution is the MILD combustion method, a recent advancement in clean combustion technologies. However, due to the limited research on MILD combustion, there is still a lack of understanding regarding its combustion

characteristics. By studying current MILD technologies, this research aims to perform an in-depth investigation into the effect of a wide range of geometry factors on the achievement of the MILD condition. These geometries include cyclonic and swirl generator blades with a wide range of blade numbers and angles. This is achieved through the utilization of CFD simulation with statistical DoE tools to evaluate the significance of each variable using a full factorial analysis approach. Finally, the design optimizer tool will be used to determine the optimum MILD combustor geometry to achieve complete PG combustion with low pollutant emissions.

## 2. Methods and Material

### 2.1 Fuel

For the production of low-grade, diluted producer gas (PG), standard air-gasification of wood-based biomass was utilized. The MILD combustion chamber will be optimized for a PG with a lower heating value (LHV) in the range of 4–6 MJ/m<sup>3</sup>. The mole fractions of the PG in Table 1 are based on an experiment by Hollingdale *et al.*, [9], which determined the composition of a combustible PG with the lowest possible quality, having an LHV of 3.99 MJ/m<sup>3</sup>.

**Table 1**

Compositions of biomass producer gas

Gas	Mole Fraction
H <sub>2</sub>	0.05
CO <sub>2</sub>	0.021
O <sub>2</sub>	0.009
N <sub>2</sub>	0.625
CH <sub>4</sub>	0.003
CO	0.292

### 2.2 Chamber Optimization

The current chamber design introduces air through a tangential inlet, while the fuel is injected via an air swirler located at the reactor bottom. Both air and fuel are injected at high velocities from the bottom upwards, generating a reversal flow that promotes gas recirculation within the chamber. The research workflow has been systematically outlined, beginning with an initial design optimization (DoE 1) and culminating in the Response Optimizer results from the second stage of optimization (DoE 2). The first step was to draft an initial design for the MILD combustion chamber, drawing on existing literature on similar designs. Simulations were conducted using ANSYS-Fluent to assess whether MILD conditions were achieved. The design and operating conditions were adjusted until the chamber met all MILD criteria. Subsequently, the design was optimized by focusing on key variables that influence MILD conditions, particularly the chamber's and swirler's geometry, based on the referenced studies. Initial values for these variables were also set according to the referenced studies. If MILD conditions were not achieved with these initial values, the geometries and operating conditions were further refined until MILD was re-established. Once MILD was achieved, suitable ranges for the variables were defined and applied to the design. Simulations were then conducted for all possible combinations of variables within these ranges until the limits of MILD combustion were identified. The results from the DoE stage were analyzed in Minitab using a full factorial approach to evaluate the significance of the geometrical variables on the response variables. This evaluation provides comprehensive information regarding the main effects, which are the influences

of individual factors, as well as the interaction effects, which are the combined influences of factors [10].

The Response Optimizer was subsequently applied across all three stages of DoE to identify the combination of significant variables that would yield the most optimal MILD performance. The final design of the MILD combustion chamber was thus optimized to minimize resource use and pollutant production. The complete methodology of the study is illustrated in Figure 1.

Each stage of the Design of Experiments (DoE) was conducted using two factors, each following a 3-level design. Simulations and analyses were performed for every possible combination of these factor levels. A 3-level general full factorial design has limitations in fully exploring the entire factor space, effective in identifying significant trends within the three levels, which can serve as a foundation for further research.

In this study, the geometric variables investigated include the combustion chamber's length ( $L_c$ ), diameter ( $D_c$ ), swirler's angle ( $\Theta_{\text{swirler}}$ ), and the number of blades on the swirler ( $N_{\text{blades}}$ ). The parameters for these variables range as follows: 500–1000 mm for  $L_c$ , 150–200 mm for  $D_c$ , 15–45° for  $\Theta_{\text{swirler}}$ , and 8–14 for  $N$  blades. The outputs measured from the simulations include CO and NOx emissions, the maximum temperature increase within the chamber, and the Damköhler number. The DoE analysis enables the evaluation of the significance of these geometric variables on the outputs, facilitating the design of an optimized MILD combustion chamber. The detailed simulation setups are provided in Table 2.

**Table 2**  
Simulations set-up for DoE 1 and DoE 2

S/no	DoE 1		DoE 2	
	$L_c$ (mm)	$D_c$ (mm)	$\Theta$ (°)	N
1	500	150	30	4
2	500	175	30	8
3	500	200	30	12
4	750	150	45	4
5	750	175	45	8
6	750	200	45	12
7	1000	150	60	4
8	1000	175	60	8
9	1000	200	60	12

The initial design of the combustion chamber and swirler was created using SOLIDWORKS, with simple geometric modifications, such as adjusting the chamber's length and diameter, performed in ANSYS SpaceClaim for convenience. Complex geometries like the swirler were modified directly in SOLIDWORKS. The simulation model was fully solid to ensure proper recognition of fluid domains by ANSYS Fluent during CFD calculations.

The initial chamber dimensions were set to 1000 mm in length and 200 mm in diameter, drawing from [11] study, which found that a cylindrical MILD combustion chamber is more effective than a cuboid design due to improved turbulent flow and better MILD performance. The tangential inlet was designed with a diameter of 0.02 m, based on Chanphavong and Phonhalath's [12] findings that this size promotes cyclonic flow and high-velocity fluid injection, increasing internal gas recirculation—an essential factor for achieving flameless MILD combustion. Despite the potential risks of high turbulence and local flame extinction associated with a smaller inlet, the 0.02 m diameter was chosen for this study based on its suitability in trial simulations.

The chamber design integrates tangential and swirling fluid injection to study the effects on turbulence and MILD conditions. Swirler's inlet dimension relies on the chamber diameter, with a

consistent 50 kW input power and steady mass flow rates for both air and fuel. The design also features high-velocity fluid injection from the bottom to the top, creating a reversal flow and promoting gas recirculation within the chamber. An outlet pipe with a 50 mm diameter was added at the top to expel exhaust gases as shown in the design dimensions detailed in Figure 1 and Table 3.

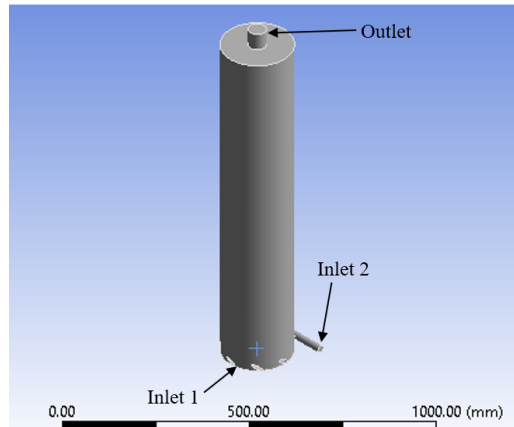


**Fig. 1.** Design of combustion chamber

The swirler's geometries were designed based on cross-referencing various literature of MILD combustion study that utilizes swirler in their chamber such as one by Zhen and Al-Attab [6] and another by Mohapatra *et al.*, [13]. The width of the blade was set as 0.01 m while its length is set as 0.35 m according to the dimensions and geometries of the swirler in Figure 2 and Table 3. The blade's height depends on the diameter of the chamber because it needs to cover the entire width of the chamber. The blades are angled towards the tangential inlet, counterflow against the cyclonic flow produced in order to maximize turbulence.

**Table 3**  
 Dimensions of combustion chamber and swirler

	Combustion Chamber	Swirler
Outlet	Length = 100 mm Diameter = 50 mm	Blade Width = 10 mm
Chamber	Length = 1000 mm Diameter = 200 mm	Blade Length = 35 mm
Inlet 1	Length = Lc = 1000 mm Diameter = Dc = 200 mm	Blade Height = Dc
Inlet 2	Diameter = 20 mm	Blade Angle = $\Theta_{\text{swirler}}$ Blade Number = N blades

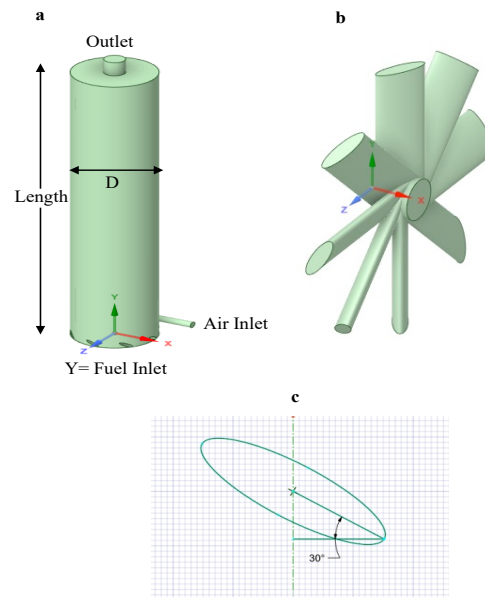


**Fig. 2.** (a) Chamber geometry, (b) Swirler geometry, (c) Swirler angle

### 2.3 CFD Modelling

In this study, 3D models for all the geometry cases dictated by DoE optimization were constructed using SOLIDWORKS. These geometries were then exported to the ANSYS Fluent workbench for mesh generation, followed by Computational Fluid Dynamics (CFD) simulations. The simulation results were manually recorded into DoE tables for analysis.

After importing the geometry into ANSYS Fluent, the first crucial step was meshing, a pivotal phase in the CFD process. The quality of the mesh is critical as it forms the basis for accurate computational analysis. The grid, composed of cells or elements created during meshing, is essential for solving fluid flow equations. The grid size directly influences computational time and, consequently, the cost of simulations. It also significantly affects convergence rates and solution accuracy. Key metrics for assessing mesh quality include skewness and aspect ratio.

A maximum skewness value above 0.98 can cause divergence errors, disrupting the convergence of the solution. The aspect ratio, defined as the ratio of the longest edge length to the shortest, ideally should be 1.0, indicating an optimal geometric configuration. Evaluating these metrics is vital to ensure robust numerical simulations. A mesh independence test, discussed later in the results section, was performed to ensure reliable and consistent simulation outcomes.

The standard  $k-\epsilon$  model was employed to replicate turbulent flow conditions within the combustor due to its proven effectiveness in predicting turbulence behavior in combustion and heat transfer simulations. This model operates based on transport equations for turbulence kinetic energy ( $k$ ) and its dissipation rate ( $\epsilon$ ), assuming fully turbulent flow and negligible molecular viscosity effects.

For the combustion modelling, the partially premixed combustion model was selected for its superior performance, incorporating a probability density function (PDF) to predefine the fuel and oxidizer species, thereby setting the composition of producer gas (PG) and air before simulation. This model can also fully separate air and fuel streams, similar to a nonpremixed combustion model, providing greater simulation flexibility. In turbulent combustion with rapid chemistry, the thermochemical state of the fluid can be characterized by a conserved scalar known as the mixture fraction, calculated using a specific equation for a fuel/oxidizer binary system. The Mean Mixture Fraction (MMF), a special case of the mixture fraction, serves as an indicator of air-fuel mixing quality, with values starting at 1 for 100% fuel concentration and decreasing as dilutants are present.

The boundary conditions outlined in Table 4 were essential for setting predefined simulation constraints and operational parameters. These conditions, derived from a test run achieving MILD combustion, remained constant across all simulations for both DoE stages combustors. The mass flow rate of fuel was fixed based on a thermal input scale of 50 kW, calculated using the LHV value for PG. The key indicator for achieving MILD combustion is the Damköhler number, a dimensionless ratio of the characteristic mixing time to the chemical reaction time. Values between 0.01 and 5.35 indicate a regime influenced by both flow and chemical time scales.

Residence time is a crucial factor as well in combustion performance, it is the time available for the fuel molecules to break down and interact with oxidizer molecules. Turns [14] use the equation below to estimate the mean residence time ( $t_m$ ) as:

$$t_m = \frac{pV}{m}$$

The mean residence time ( $t_m$ ) is calculated using the average gas density ( $\rho$ ), the total chamber volume ( $V$ ), and the total mass flow ( $m$ ). The total chamber volume, influenced by the chamber's diameter, length, and height, is a primary factor affecting residence time.

**Table 4**  
 Boundary conditions of simulated combustors

Air inlet	Velocity	31.024 m/s
	Mass flow rate	0.012602272 kg/s
	Initial gauge pressure	0 atm
	Temperature	473 K
	Mean mixture fraction	0
Fuel inlets	Velocity	39.89 m/s
	Mass flow rate	0.00610202 kg/s
	Initial gauge pressure	0 atm
	Temperature	673 K
	Mean mixture fraction	1
Pressure outlet	Back flow temperature	1000 K

### 3. Results and Discussion

#### 3.1 Model Validation and Grid Independence Test

The temperature values of the CFD simulation model were compared with the CFD and experimental findings from Orsino *et al.*, [15] on an industrial axial furnace of square cross-section (2m × 2m) with a chamber length of 6.25m. The setup included high velocity injectors of central hot air jet (at 1300°C and 85m/s) surrounded by gas fuel jet injectors (at 100m/s). The exact combustion chamber geometry of the reference work was analysed to assess the applicability of the current CFD setting in the current work, including a partially premixed combustion model (with pdf) along with k-ε model for MILD combustion attainment. In the reference study, additional to the experimental work, the combustor was also simulated using a non-premixed combustion model [15]. Temperature values along the radial distance of 1m from the chamber centre axis to the outer wall were recorded for the reference study [15] and compared to the verification results from the current study CFD simulation as shown in Figure 3a. Temperature values predicted by CFD modelling were within the range of the reference work's CFD and experiment results. The fuel injection zone (0.28m) and its surroundings (0.1-0.35m) posed a classical challenge to the CFD modelling at the “beyond rich flammability limit” zone where no combustion occur, along with its boundaries where the reaction is initiated. The prediction from the model depends mainly on the rich flammability limit setup where

both CFD models from the current model and the reference model expanded this non-combustion zone towards the chamber centre where air is injected, while experimental results showed that combustion started to propagate at this zone. However, this is highly dependent on the fuel type, purity, etc., where the estimated rich flammability limit might deviate from the actual experimental value, which is difficult to predict as fuel properties in practice are not consistent. However, at normal mixtures (stoichiometric-to-slightly lean) the predictions from both CFD models showed high agreement with the experimental data with low difference of 1.7%, which indicates that this CFD model setting can reliably predict combustion reaction inside the chamber.

A Grid Dependency Test (GDT), also known as a grid independence test, is conducted to determine the highest acceptable mesh quality without exceeding the computational limits of the hardware. In CFD simulations, the mesh needs to be refined enough to produce accurate results; however, finer meshes generally require longer generation times, which in turn increase the overall simulation time. Conversely, a coarser mesh, while quicker to generate, may lead to significantly less accurate and potentially faulty results. This occurs because the smaller the mesh size, the closer the approximate solution will be to the true solution. Therefore, the GDT is essential to strike a balance between mesh quality and computational efficiency, determining the optimal mesh size for the model.

The GDT was performed by varying the element size within a range of 0.003 to 0.05 as seen in Table 5, resulting in a mesh with 878,752 to 2,656,795 elements. The key parameter tested across this range was the maximum outflow temperature at the chamber's outlet. As illustrated in Figure 3b, beginning with an element size of 0.05, the outflow temperature increased gradually, reaching a peak of 1621.87 K at an element size of 0.01. Beyond this point, the outflow temperature decreased to 1614.74 K at an element size of 0.0075, followed by a slight rise to 1618.02 K at an element size of 0.005. After this, the outflow temperature stabilized, with fluctuations of only  $\pm 0.01\%$  observed for smaller element sizes. Based on these findings, an element size of 0.005, corresponding to 1,717,939 elements, was selected as the optimal mesh size for the remainder of the simulations.

**Table 5**  
 Grid dependency test results of the simulations

	Number of Elements	Outlet Temperature (K)	Fluctuation (%)
0.05	878752	1613.47	-
0.025	1058187	1620.30	0.42
0.01	1174209	1621.87	0.10
0.0075	1294753	1614.74	-0.44
0.005	1717939	1618.02	0.20
0.004	2187367	1617.88	-0.01
0.003	2656795	1617.99	0.01

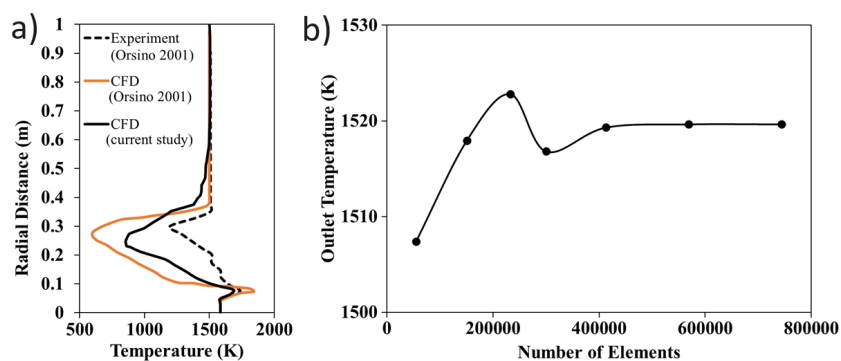


**Fig. 3.** (a) CFD model verification (b) Grid dependency test

### 3.2 DoE 1 Optimization

DoE 1 focuses on optimizing the geometry of the MILD combustion chamber, specifically its length (Lc) and diameter (Dc). This optimization was conducted based on the results from 9 simulations, each corresponding to a different combination of Lc and Dc.

The primary response variables targeted for optimization include the maximum temperature increase ( $\Delta T$ ), the Damköhler number (Da), and pollutant emissions (CO & NOx). The  $\Delta T$  was calculated as the difference between the maximum temperature within the chamber and the inlet temperature, Da was derived from the mixing zone of the reactants, and pollutant emissions were measured at the chamber's outlet.

The binary outcome of whether the chamber achieved MILD combustion was coded as 1 for YES and 0 for NO, ensuring that chambers not meeting MILD conditions were excluded from further analysis in Minitab. The results of these simulations, along with the corresponding inputs and response variables, are detailed in Table 6.

**Table 6**  
 Results of DoE 1

Lc (mm)	Dc (mm)	$\Delta T$ (°C)	Da	CO (ppm)	NOx (ppm)	MILD
500	150	859.08	0.2183	2226.00	252.00	0
500	175	1134.49	0.2518	4907.00	135.00	0
500	200	439.62	0.2877	2929.00	16.33	1
750	150	935.08	0.2141	873.00	324.00	0
750	175	649.77	0.2930	4782.00	38.49	1
750	200	483.24	0.2944	1190.00	15.19	1
1000	150	972.40	0.2133	337.00	208.00	0
1000	175	606.64	0.2741	3230.00	178.00	1
1000	200	333.45	0.2991	1969.77	15.46	1

### 3.3 Effect of Combustor Geometry

The analysis of relationship between the chamber's diameter (Dc) and various variables is explained deeply in the corresponding graphs. In this regard, the temperature increase ( $\Delta T$ ) at a chamber length of 500 mm is shown in Figure 4a, b and c, and thus, only the 200 mm diameter meets the requirement of  $T_{si} < 750^\circ\text{C}$ , making it the sole configuration that achieves the MILD condition.

While, Figure 4b illustrates that Da gradually increases as the diameter widens, and for the pollutant emissions, at 150 mm chamber diameter, very high CO emissions of 2226 ppm steady increases to 4907 ppm at 175 mm and then falls to 2929 ppm at 200 mm, while NOx emissions decrease steadily as the diameter increases from 252 to 16.33 ppm as reveals in Figure 4c.

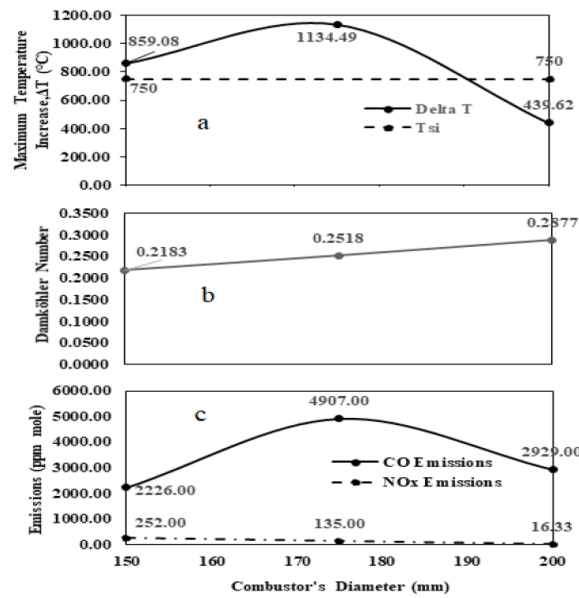


**Fig. 4.** (a) Graph of  $\Delta T$  against  $D_c$ , (b) Graph of  $Da$  against  $D_c$  and (c) Graph of Pollutants Emissions against  $D_c$  for  $LC=500mm$

Both the 175 mm and 200 mm diameters fulfil the  $T_{si} < 750^\circ C$  criterion for a length of 750 mm, therefore, signifying that these are the only configurations that reach the MILD condition in the chamber, as depicted in Figure 5a, where  $\Delta T$  decreases as the diameter increases.

Similarly, for a chamber length of 1000 mm, only the 175 mm and 200 mm diameters meet the  $T_{si} < 750^\circ C$  requirement, with the 150 mm diameter failing to achieve MILD across all tested geometries. Figure 5b shows that  $Da$  increases when the diameter changes from 150 mm to 175 mm but then plateaus at 200 mm.

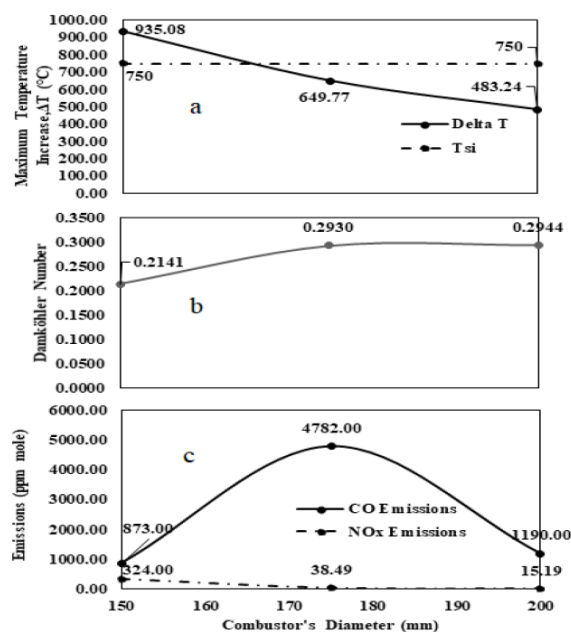


**Fig. 5.** (a) Graph of  $\Delta T$  against  $D_c$ , (b) Graph of  $Da$  against  $D_c$  and (c) Graph of pollutants emissions against  $D_c$  for  $LC=750mm$

Furthermore, in 1000 mm chamber,  $\Delta T$  decreases as the diameter widens, indicating an inverse relationship between  $\Delta T$  and  $D_c$  as shown from Figure 6a. Regarding the Damköhler number ( $Da$ ), all

tested geometric combinations satisfy the  $0.01 < Da < 5$  requirement. Figure 6b shows a noticeable rise in  $Da$  from 150 mm to 175 mm, with the rate of increase slowing as the diameter grows and this suggests that  $Da$  increases with an increase in diameter.

A similar trend is observed for two chamber lengths of 750 mm and 1000 mm shown in Figures 5c and 6c respectively. Given that all configurations with a 150 mm diameter failed to achieve MILD.

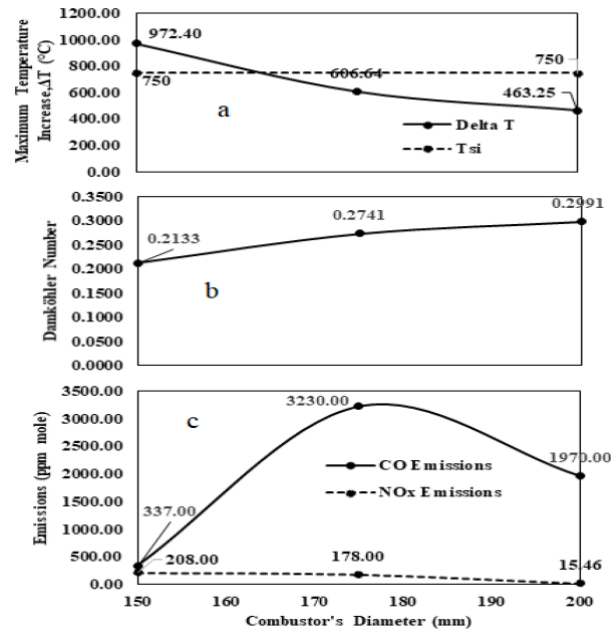


**Fig. 6.** (a) Graph of  $\Delta T$  against  $D_c$ , (b) Graph of  $Da$  against  $D_c$  and (c) Graph of pollutants emissions against  $D_c$  for  $LC=1000mm$

By synthesizing the relationships between parameters and variables, a clearer understanding emerges of how combustor geometry influences MILD combustion conditions. Figures 4a, 5a, and 6a illustrate the impact of chamber diameter ( $D_c$ ) on temperature increase ( $\Delta T$ ). Chambers that did not achieve MILD generally exhibit higher  $\Delta T$  values, which decrease as the chamber diameter increases.

This inverse relationship is mirrored by the Damköhler number ( $Da$ ) in Figures 4b, 5b, and 6b, indicating that a higher  $\Delta T$  correlates with a lower  $Da$  and vice versa. Additionally, Figures 4c, 5c, and 6c show a peak in CO emissions for the 175 mm diameter combustor, while NOx emissions decrease as  $D_c$  increases.

As the combustor widens, the increased volume affects residence time, a critical factor in combustion. A larger chamber volume provides more space for reactants to mix and diffuse, slowing reaction rates and extending residence time. This allows for more complete combustion, leading to better mixing, higher  $Da$ , and reduced CO and NOx emissions at the outlet. Enhanced mixing also distributes combustion more evenly throughout the chamber, resulting in a lower maximum temperature increase. The same principle applies to chamber length, where a longer chamber further increases residence time. Therefore, for achieving MILD combustion, an increased chamber volume optimizes performance by improving residence time and reactant mixing. Thus, theoretically, the most optimal design would be a chamber with the largest volume, such as  $D_c = 200$  mm and  $LC = 1000$  mm.

### 3.4 Optimum Geometry for DoE 1

The Response Optimizer in Minitab was employed on DoE 1 to identify the optimal combination from the simulations. Specific targets and constraints were applied to the responses to ensure that only desirable outcomes were included in the optimization process.

In the Response Optimizer settings, the MILD response was set to "Maximize," ensuring that only configurations achieving MILD combustion were considered. For CO and NO<sub>x</sub> emissions, the goal was set to "Minimize," aligning with the project's aim to design a combustion chamber that minimizes pollutant production. The Damköhler number (Da) response was set to "Target" with a value of 1.0, as this represents the ideal point where the fuel-air mixture approaches unity. Lastly, ΔT was set to "Minimize" to exclude configurations where ΔT exceeds 750°C, as these do not meet the MILD combustion criteria. The resulting optimization plot for the chamber's geometry is presented in Figure 7.

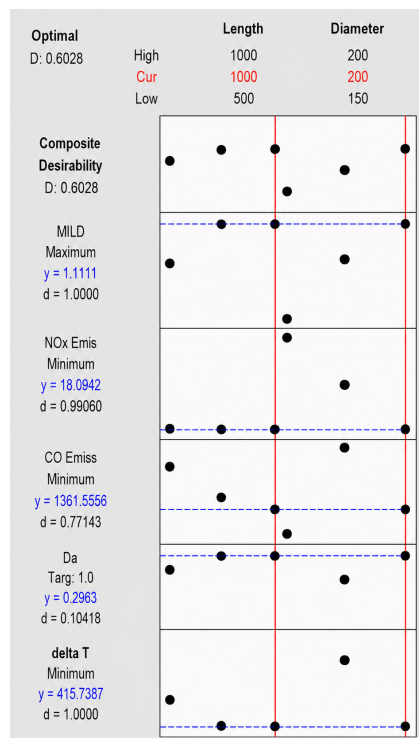


Fig. 7. Optimization plot of DoE 1

Desirability is a score assigned to a set of responses that indicates how close they are to the ideal outcome. It ranges from zero to one, with zero representing the worst case and one representing the ideal. Ideally, desirability should fall between 0.8 and 1.0 to be considered optimal, but values above 0.5 are still deemed acceptable. In the Response Optimizer, two types of desirability are calculated: Individual Desirability, which measures how closely each response meets the target, and Composite Desirability, which aggregates the individual scores into an overall value reflecting how ideal the case is. The optimizer calculates the estimated fitted values (y) for each variable, with the geometry that yields response values closest to these fitted values being considered optimal. For this case, the fitted values are: 1.1111 for MILD, 18.0942 for NO<sub>x</sub> emissions, 1381.5556 for CO emissions, 0.2953 for the Damköhler number (Da), and 415.7387 for ΔT. Based on the optimization plot, the individual desirability for the MILD response and ΔT is 1.0, indicating that the optimal case successfully achieved MILD combustion with a low ΔT. The individual desirability for CO and NO<sub>x</sub> emissions is 0.77143 and 0.99060, respectively, showing that pollutant emissions are minimized to an acceptable level. However, the Da has the lowest individual desirability of 0.10418, suggesting that the mixture is far from ideal in terms of achieving unity. Overall, the composite desirability for the optimal case is

calculated to be 0.6028, which is considered reliable. The geometry determined to be the most optimal by the Response Optimizer is a combustion chamber with a length ( $L_c$ ) of 1000 mm and a diameter ( $D_c$ ) of 200 mm. The model of this optimal chamber geometry is shown in Figure 8.



Fig. 8. Model of optimal combustion chamber geometry

### 3.5 DoE 2 Optimization

The second stage Design of Experiments (DoE 2) focuses on optimizing the geometry of the swirler in the MILD combustion chamber, specifically its angle ( $\Theta_{\text{swirler}}$ ) and the number of blades (Nblades). This optimization was based on the results from nine simulations, each representing different combinations of  $\Theta_{\text{swirler}}$  and Nblades. Similar to DoE 1, the primary response variables optimized were the maximum temperature increase ( $\Delta T$ ), the Damköhler number (Da), and pollutant emissions (CO & NO<sub>x</sub>). The simulation results, along with the corresponding input parameters and responses, are presented in Table 7 below.

**Table 7**  
 Results of DoE 2

$\Theta$ (°)	N	$\Delta T$ (°C)	Da	CO (ppm)	NO <sub>x</sub> (ppm)	MILD
30	4	128.54	0.5824	10.45	59.93	0
30	8	333.45	0.2991	0.74	15.46	1
30	12	218.45	0.4425	1.5	26.12	0
45	4	169.42	0.3048	0.32	84.96	0
45	8	385.60	0.2272	0.29	30.70	1
45	12	336.95	0.2663	0.58	76.97	1
60	4	251.89	0.4513	51.1	124.08	0
60	8	606.57	0.3390	22.34	90.39	1
60	12	372.70	0.4292	0.445	102.96	1

### 3.6 Effect of DoE 2 Combustor Geometry

The relationship between the swirler angle ( $\Theta$ ) and various variables was analyzed through a series of graphs. For both the 4-bladed and 8-bladed swirlers, each tested  $\Theta$  met the requirement of  $\Delta T < T_{si}$ , with  $\Delta T$  gradually increasing as the angle is increased, as shown in Figures 9a and 10a. However, for the 12-bladed swirler, as seen in Figure 11a, while it also fulfilled the MILD combustion criteria, the  $\Delta T$  followed a different trend, rising steadily from 30° to 45° and then plateauing at 60°. Overall, it can be concluded that the  $\Delta T$  and  $\Theta$  are generally directly proportional. Regarding the Damköhler number (Da), Figures 9b, 10b, and 11b display a downward trend, with the Da decreasing

at 45° and increasing at 60°. This pattern is consistent across all tested blade numbers (N). Therefore, it can be inferred that Da tends to rise as the swirler angle (Θ) approaches either extreme.

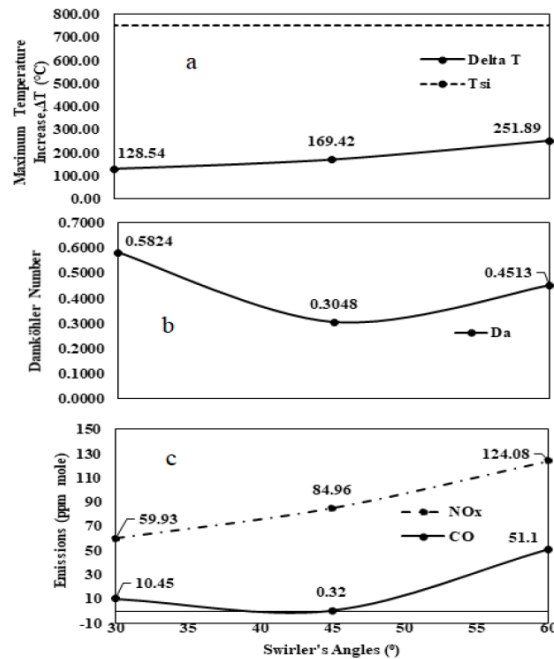


Fig. 9. (a) Graph of  $\Delta T$  against  $\Theta$ ; (b): Graph of Da against  $\Theta$ ; (c) Graph of pollutants emissions  $\Theta$  for N= 4

In terms of pollutant emissions, Figures 9c and 10c indicate that for the 4-bladed and 8-bladed swirlers, both CO and NOx emissions (in ppm) increase progressively with the swirler angle ( $\Theta$ ), with a more pronounced rise observed beyond 45°.

However, as shown in Figure 11c, the 12-bladed swirler exhibits a different behavior. While NOx follows the same increasing trend, CO emissions display an inverse relationship, decreasing exponentially between 30° and 45°, and then stabilizing with a smaller variation at 60°. Overall, CO and NOx emissions generally increase with the swirler angle, except in the case of the 12-bladed swirler, where CO emissions decline as the swirler angle increases.

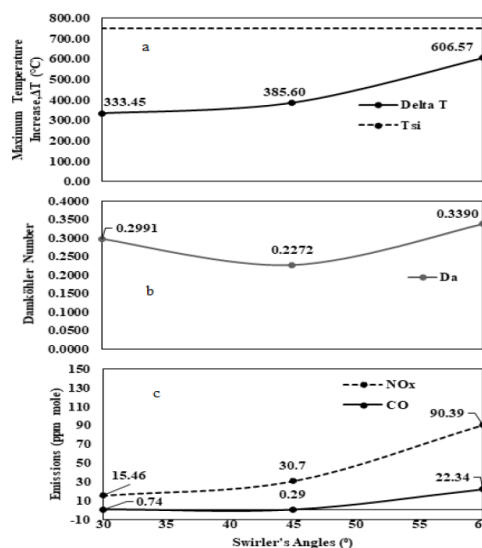
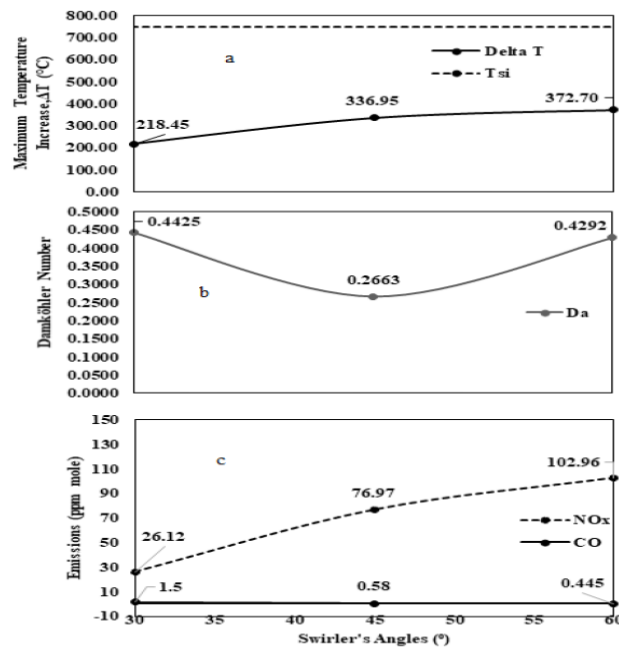


Fig. 10. (a) Graph of  $\Delta T$  against  $\Theta$ ; (b): Graph of Da against  $\Theta$ ; (c) Graph of pollutants emissions  $\Theta$  for N= 8

By analyzing the information obtained from the ANOVA and establishing the relationships between the parameters and variables, further insights can be drawn into the influence of swirler

geometry on MILD combustion conditions. Figures 9a, 10a, and 11a illustrate that as the swirler angle ( $\Theta$ ) increases, there is a corresponding rise in  $\Delta T$ , which is directly linked to an increase in NOx emissions, as evidenced in Figures 9c, 10c, and 11c. Thus, higher swirler angles result in increased  $\Delta T$  and NOx emissions. The Damköhler number (Da) for all three swirler configurations exhibits a downward trend, with a minimum occurring at  $45^\circ$ , as shown in Figures 9b, 10b, and 11b. This suggests that as the angle approaches  $0^\circ$  or  $90^\circ$ , Da will increase, provided the angle generates sufficient swirling motion. However, the behaviour of CO emissions is more complex. Figures 9c and 10c show that CO emissions decrease sharply to a minimum as the swirler angle increases from  $30^\circ$  to  $45^\circ$ , where emissions are the lowest, then CO emissions rise significantly, peaking at the  $60^\circ$  swirler angle. Figure 11c indicates that for a 12-bladed swirler, CO emissions are very low overall with a consistent decrease from 1.5 ppm at  $30^\circ$  to 0.445 ppm at  $60^\circ$  as the swirler angle increases, likely due to changes in the swirl dynamics as the number of blades increases.



**Fig. 11.** (a) Graph of  $\Delta T$  against  $\Theta$ ; (b): Graph of Da against  $\Theta$ ; (c) Graph of pollutants emissions  $\Theta$  for  $N = 12$

The primary function of a swirler in the combustion chamber is to generate a swirling vortex that moves counter to the tangential inlet flow. In theory, this interaction creates turbulence that promotes molecular-level mixing of reactants, slowing down the flow to allow for more complete combustion. A lower swirler angle is expected to increase the contact area between the fuel and the swirler, thereby enhancing the centrifugal forces acting on the fuel and producing a stronger vortex. The number of blades on the swirler also plays a crucial role in either intensifying or weakening this vortex. A greater number of blades increases the contact area between the fuel and the swirler, leading to a more chaotic flow, which enhances fuel-air mixing and increases the likelihood of complete combustion. As the swirler angle deviates from  $45^\circ$ , increasing or decreasing, the flow field becomes more turbulent. This increases the surface area over which the fuel and air interact, thereby improving mixing and accelerating the reaction rate, reflected in a higher Damköhler number (Da). Additionally, the increased exposure of fuel to air enhances the heat transfer rate, resulting in a higher  $\Delta T$ . Better fuel-air mixing also accelerates fuel decomposition, leading to reduced CO emissions and lower thermal NOx formation. In conclusion, the swirler design that generates the most vigorous vortex yields optimal results by improving reactant mixing through chaotic flow fields.

Therefore, it can be inferred that the most effective design likely involves 8 to 12 blades and a swirler angle either below or above 45°.

### 3.6 Optimum Geometry for DoE 2

To identify the optimal combinations from the simulation results, the Response Optimizer was applied to the DoE 2 data. Similar to the approach used in DoE 1, the same targets and constraints were established for this optimization process. The resulting optimization plot for the swirler's geometry is presented in Figure 12.

The calculated y-values for each variable are 11.4011 for NOx emissions, 2.2683 for CO emissions, 0.3585 for the Damköhler number (Da), and 357.1789 for ΔT. According to the optimization plot, the individual desirability for ΔT is 0.81349, indicating that the optimal case yields the lowest ΔT among all cases that achieve MILD combustion. The individual desirability for CO and NOx emissions are 0.96106 and 1.0, respectively, suggesting that the pollutant emissions in the optimal case are relatively low and well-controlled. However, the Da individual desirability is the highest at 0.963, indicating that the optimal case is close to achieving a unity mixture. Combining the individual desirability values, the composite desirability for the optimal case is calculated to be 0.9316, which is considered strongly reliable. The Response Optimizer identified the most optimal swirler geometry as having a swirler angle (Θ<sub>swirler</sub>) of 30° and 8 blades.

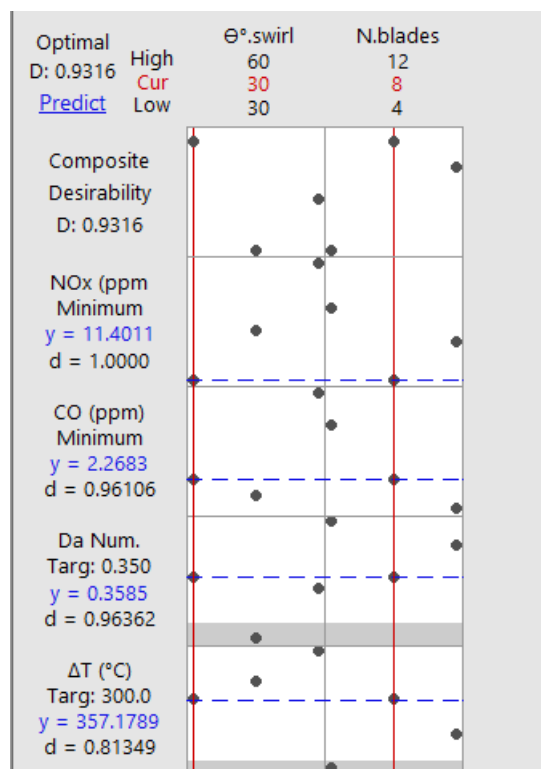


Fig. 12. Optimization plot for DoE 2

### 3.6 Optimum Condition Performance Analysis

ANSYS simulations results highlight that the selected swirler geometry, featuring a 30° swirler angle and 8 blades, provides an optimal balance between emission control and combustion efficiency, reflected in a high composite desirability score of 0.9316. The configuration minimizes NOx emissions, achieving a value of 11.4011 ppm with a perfect desirability score of 1.0000.

Additionally, CO emissions are kept low at 2.2683 ppm, with a desirability score of 0.96106, demonstrating effective control over incomplete combustion. The Damköhler number (Da), measured at 0.3585, less than one, with a desirability score of 0.96362, indicating that the balance between reaction time and mixing time is well-optimized, ensuring efficient combustion.

The maximum temperature increase ( $\Delta T$ ) reached 357.1789 °C, and the desirability score of 0.81349 suggests that the temperature remains within acceptable limits below the self-ignition temperature, complying with the MILD combustion condition. This slight increase in temperature could be attributed to the enhanced combustion efficiency resulting from better fuel-air mixing provided by the chosen swirler geometry. In terms of performance, the selected combination of a 30° swirler angle and 8 blades strikes an ideal balance between mixing intensity and combustion stability. The 30° swirler angle generates sufficient turbulence for effective fuel-air interaction without causing excessive disruption in the combustion flow, which could destabilize the flame or increase emissions. The 8-blade configuration enhances swirling, promoting better mixing and ensuring more complete combustion, thus minimizing CO emissions and keeping thermal NO<sub>x</sub> within acceptable levels. Overall, the optimum condition provides a robust solution that maintains efficient combustion, effectively controls pollutant emissions, and ensures stable flame behavior, making it a highly effective configuration for achieving MILD combustion conditions. Therefore, ANSYS simulation results clearly reveal in Figure 13, a, b and c the respective temperature, axial velocity and residence time path line contours of optimal design.

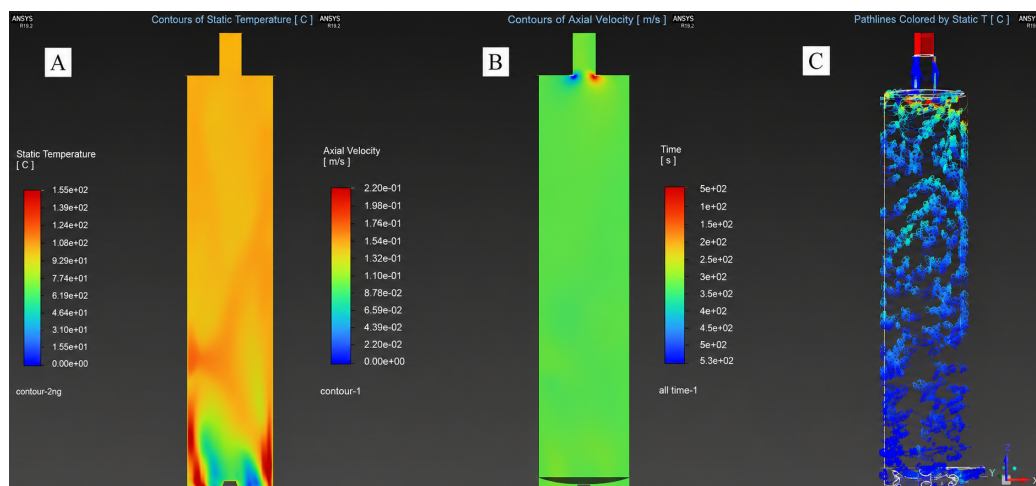


**Fig. 13.** (a) Temperature, (b) Axial velocity and (c) Residence time path line contours of optimal design

#### 4. Conclusions

The project objectives in determining the optimal chamber and swirler geometry for a MILD combustion chamber fuelled by low-grade, biomass-derived producer gas were successfully achieved. A two-stage DoE was conducted to optimize the cylindrical chamber design, focusing on chamber length, diameter, swirler angle, and number of blades. In total, 18 CFD simulations were performed in ANSYS Fluent following the DoE plan in Minitab, with 9 simulations per DoE stage, testing two geometric parameters with three levels each. The optimization process through DoE 1 and DoE 2 was essential to identify the ideal MILD combustor geometry. DoE 1 focused on optimizing the chamber's dimensions, specifically the diameter ( $D_c$ ) and length ( $L_c$ ), leading to a  $D_c$  of 200 mm and  $L_c$  of 1000 mm as the optimal configuration. This combination produced relatively low NO<sub>x</sub> emissions and an acceptable Damköhler number (Da), indicating effective mixing and combustion stability. The results of DOE 1 highlighted that both chamber dimensions significantly influenced in

high CO emissions, while only Dc impacted NOx emissions and Da, providing a foundational chamber design for effective MILD combustion. DoE 2 further refined this design by optimizing the swirler parameters angle ( $\Theta$ ) and number of blades (N) to enhance fuel-air mixing within the chamber. The optimal swirler configuration, with a 30° angle and 8 blades, minimized CO emissions significantly while maintaining NOx emissions at a low level, indicating improved combustion efficiency and pollutant control. Statistical analysis from DoE 2 showed that both swirler parameters significantly impacted  $\Delta T$ , NOx, and CO emissions, confirming their critical role in achieving complete combustion. The combined results of DoE 1 and DoE 2 established the final optimal model, integrating the best chamber dimensions and swirler configuration to achieve the most efficient combustion performance with minimal pollutant emissions.

### Acknowledgment

The authors express their gratitude to Universiti Sains Malaysia for providing the facilities and software support for this study, and also would like to thank the MRUN Translational Research Grant (USM-MTUN-MCUN) with grant number 304/PJKIMIA/656501/K145 for the financial support.

### References

- [1] Capellán-Pérez, Iñigo, Margarita Mediavilla, Carlos de Castro, Óscar Carpintero, and Luis Javier Miguel. "Fossil fuel depletion and socio-economic scenarios: An integrated approach." *Energy* 77 (2014): 641-666. doi: [10.1016/j.energy.2014.09.063](https://doi.org/10.1016/j.energy.2014.09.063).
- [2] Shafiee, Shahriar, and Erkan Topal. "When will fossil fuel reserves be diminished?." *Energy policy* 37, no. 1 (2009): 181-189. doi: [10.1016/j.enpol.2008.08.016](https://doi.org/10.1016/j.enpol.2008.08.016).
- [3] International Energy Agency (IEA), "Electricity Market Report 2023," IEA, 2023. [Online]. Available: <https://www.iea.org/reports/electricity-market-report-2023/executive-summary>
- [4] J. Oakey, *Fuel Flexible Energy Generation: Solid, Liquid and Gaseous Fuels (Woodhead Publishing Series in Energy)*, 1st ed. Woodhead Publishing, 2015.
- [5] Chanphavong, Lemthong, Khaled A. Al-attab, and Zainal Alimuddin Zainal. "Swirl flow field analysis of producer gas premixed charge in a flameless cyclone combustor." *International Journal of Energy Research* 42, no. 14 (2018): 4360-4371. doi: [10.1002/er.4174](https://doi.org/10.1002/er.4174).
- [6] Zhien, Chai Yik, and Khaled Ali Al-attab. "Design optimization of trio concept combustor geometry for low-grade biomass producer gas combustion." *Energy* 238 (2022): 121705. doi: [10.1016/j.energy.2021.121705](https://doi.org/10.1016/j.energy.2021.121705).
- [7] McCaffrey, Zach, Peter Thy, Michael Long, Melina Oliveira, Li Wang, Lennard Torres, Turkan Aktas, Bor-Sen Chiou, William Orts, and Bryan M. Jenkins. "Air and steam gasification of almond biomass." *Frontiers in energy research* 7 (2019): 84. doi: [10.3389/fenrg.2019.00084](https://doi.org/10.3389/fenrg.2019.00084).
- [8] Mohamed, Hamdi, Benticha Hmaeid, and Sassi Mohamed. "Fundamentals and simulation of MILD combustion." *Thermal Power Plants* (2012): 43-64. doi: [10.5772/27206](https://doi.org/10.5772/27206).
- [9] Hollingdale, A. C., G. R. Breag, and D. Pearce. "Producer gas fuelling of a 20 kW output engine by gasification of solid biomass." (1988): 20-pp. Available: <https://gala.gre.ac.uk/id/eprint/11057/1/Doc-0107.pdf>
- [10] Yılbaşı, Zeki. "Biofuels, e-fuels, and waste-derived fuels: advances, challenges, and future directions." *Sustainability* 17, no. 13 (2025): 6145. <https://doi.org/10.3390/su17136145>
- [11] Al Rifai, Omar, K. A. Al-attab, Ibrahim I. Enagi, K. F. Mustafa, and Abdul Rahman Mohamed. "Optimization of MILD chamber design for combustion of producer gas from biomass gasification." *Green Technologies and Sustainability* 3, no. 4 (2025): 100220. <https://doi.org/10.1016/j.grets.2025.100220>.
- [12] C. Lemthong and K. Phonhalath, "Premixed combustion of producer gas in a cyclonic flow combustion chamber under varying number of burners," *Energy Sources, Part A: Recovery, Utilization, and Environmental Effects*, 2020. doi: [10.1080/15567036.2020.1826015](https://doi.org/10.1080/15567036.2020.1826015).
- [13] Mohapatra, Subhankar, Radi Alsulami, Srinibas Karmakar, Sukanta Kumar Dash, and V. Mahendra Reddy. "Experimental and computational investigation upon combustion characteristics of liquid fuel in a novel combustor with hybrid swirl and recirculation bowl." *ACS omega* 8, no. 1 (2022): 1523-1533. doi: [10.1021/acsomega.2c07028](https://doi.org/10.1021/acsomega.2c07028).
- [14] S. R. Turns, *An Introduction to Combustion: Concepts and Applications*, 3rd ed. McGraw-Hill Education, 2012.

- [15] Orsino, Stefano, R. O. M. A. N. WEBER\*, and Ugo Bollettini. "Numerical simulation of combustion of natural gas with high-temperature air." *Combustion Science and Technology* 170, no. 1 (2001): 1-34. [doi: 10.1080/00102200108952128](https://doi.org/10.1080/00102200108952128).